

Stabilized Finite Difference Methods for the Fully Dynamic Biot's Problem*

Natalia Boal^a, Francisco J. Gaspar^a,
Francisco J. Lisbona^a and Petr N. Vabishchevich^b

^a *University of Zaragoza*

Pedro Cerbuna, 12, 50009 Zaragoza, Spain

^b *Nuclear Safety Institute*

52, B. Tulskaya, 115191 Moscow, Russia

E-mail: nboal@unizar.es

E-mail(*corresp.*): fjgaspar@unizar.es

E-mail: lisbona@unizar.es

E-mail: vabishchevich@gmail.com

Received December 27, 2012; revised July 6, 2013; published online September 1, 2013

Abstract. This paper deals with the stabilization of the poroelasticity system, in the incompressible fully dynamic case. The stabilization term is a perturbation of the equilibrium equation that allows us to use central difference schemes to approximate the first order spatial derivatives, yielding numerical solutions without oscillations independently of the chosen discretization parameters. The perturbation term is a discrete Laplacian of the forward time difference, affected by a stabilization parameter depending on the mesh size and the properties of the porous medium. In the one-dimensional case, this parameter is shown to be optimal. Some numerical experiments are presented to show the efficiency of the proposed stabilization technique.

Keywords: poroelasticity, stabilization, finite-differences, three-level schemes.

AMS Subject Classification: 65N06; 65M06; 74F10; 74S20.

1 Introduction

The mathematical equations governing the dynamic behaviour of fully saturated elastic porous media were provided by Biot [3], using the displacements of the solid phase and the fluid displacement relative to the solid phase as variables. The study of these models are of great interest in geomechanics due to their applications in the study of the earthquake response of soil structures. We focus on the fully dynamic Biot's model which describes wave propagations in Ω , a domain in \mathbb{R}^n , $n \leq 3$, occupied by an elastic, porous and permeable

* This research has been partially supported by FEDER/MCYT Projects MTM2010-16917 and the DGA (Grupo consolidado PDIE).

matrix of density ρ , saturated by a viscous and slightly compressible or incompressible fluid. For problems where high-frequency components are absent, an economical model based on the displacements $\mathbf{u}(\mathbf{x}, t)$ of the solid phase and the pore-pressure $p(\mathbf{x}, t)$ as the essential variables was proposed in [9]. This model, called $\mathbf{u} - p$ formulation, is given by the system of equations

$$\begin{aligned} \rho \frac{\partial^2 \mathbf{u}}{\partial t^2} - \mu \Delta \mathbf{u} - (\lambda + \mu) \nabla (\nabla \cdot \mathbf{u}) + \alpha \nabla p &= \mathbf{g}(\mathbf{x}, t), \\ \frac{\partial}{\partial t} (\gamma p + \alpha \nabla \cdot \mathbf{u}) - \nabla \cdot (k \nabla p) &= f(\mathbf{x}, t), \end{aligned} \quad (1.1)$$

where λ and μ are the Lamé coefficients; $\gamma = n\tilde{\gamma}$, with n the porosity and $\tilde{\gamma}$ the compressibility coefficient of the fluid; k is the conductivity defined by $k = \kappa/\eta$ with κ the permeability of the porous medium, η the viscosity of the fluid, and α is the Biot–Willis constant. Adequate initial and boundary conditions must be supplemented. The existence and uniqueness of solution of this coupled mixed hyperbolic–parabolic system has been studied in [2].

A very interesting case corresponds to the problem of a porous medium with small permeability, saturated by an incompressible fluid. The presence of non-physical oscillations in the numerical solution if finite elements with equal order polynomial interpolation spaces are used for pressure and displacements is well known. To minimize this difficulty, different interpolation spaces for displacements and pressure, satisfying the LBB condition, can be chosen. Nevertheless, in order to use simpler codes, stabilization techniques permitting equal interpolation spaces have been investigated in the past years. Stabilization methods based on adding to the pressure equation a stabilization term have been studied in [7, 10]. Although these techniques are simple, in general, they suffer from the need to know a priori the stabilization parameter. In the quasi-static Biot’s model, a stabilization term is added to the flow equation in [1], obtaining solutions without oscillations independently of the chosen discretization parameters. The stabilization parameter, which depends on the elastic properties of the solid, and on the size of the triangulation, is given a priori, and it is shown that in the one-dimensional case, this parameter is optimal.

In the framework of finite-difference methods, similar oscillatory behaviour is observed if the standard second-order central difference scheme is used to approximate the first order derivatives appearing in system (1.1). In [4] it is shown that the use of staggered grid discretizations provides solutions free of oscillations for any values of discretization parameters. For other Biot’s models, staggered grids have also been successfully applied, see for example [5, 6]. In this work, collocated grids and standard central difference schemes are considered. To remove the spurious numerical oscillations, a stabilization technique based on a well defined perturbation of the first equation of system (1.1) is proposed.

The rest of the paper is organized as follows. In Section 2, we focus on a one-dimensional problem to analyze the numerical behaviour of standard discretizations and to identify the reason of the appearing of spurious oscillations. After the analysis of this unstable behaviour, in Section 3, we propose a new stabilized finite difference scheme, and stability estimates and convergence re-

sults on suitable energy norms are obtained. We finish the paper with some numerical experiments on one and two dimensions which confirm the efficiency of the stabilization strategy.

2 The One-Dimensional Problem

Let us consider a test problem which corresponds to a column of a porous medium saturated by an incompressible fluid, bounded by impermeable and rigid lateral walls and bottom, and supporting a unit load on the top which is free to drain. Taking $\alpha = 1$ as Biot–Willis constant, this problem is modelled as a particular case of (1.1), with $\gamma = 0$ because of the incompressibility of the fluid. So, we have the following system of partial differential equations

$$\begin{aligned} \rho \frac{\partial^2 u}{\partial t^2} - (\lambda + 2\mu) \frac{\partial^2 u}{\partial x^2} + \frac{\partial p}{\partial x} &= 0, \\ \frac{\partial}{\partial t} \left(\frac{\partial u}{\partial x} \right) - k \frac{\partial^2 p}{\partial x^2} &= 0, \quad x \in (0, 1), \quad 0 < t < T \end{aligned} \tag{2.1}$$

subject to the boundary and initial conditions

$$(\lambda + 2\mu) \frac{\partial u}{\partial x}(0, t) = 1, \quad p(0, t) = 0, \quad t \in (0, T], \tag{2.2}$$

$$u(1, t) = 0, \quad \frac{\partial p}{\partial x}(1, t) = 0, \quad t \in (0, T], \tag{2.3}$$

$$u(x, 0) = 0, \quad \frac{\partial u}{\partial t}(x, 0) = 0, \quad x \in (0, 1). \tag{2.4}$$

Applying the method of separation of variables to this test problem, it is possible to calculate its analytical solution which represents damped waves for both displacement and pressure. The performance of the solution is very different depending on a relation between the parameters in the problem. So, when $k\pi\sqrt{\rho(\lambda + 2\mu)} - 1 > 0$ the solution is a damped wave with marked oscillatory behaviour, where the displacement is given by

$$u(x, t) = \sum_{n=0}^{\infty} b_n \cos(m_n x) e^{-at} \left(\cos(\sqrt{d_n} t) + \frac{a}{\sqrt{d_n}} \sin(\sqrt{d_n} t) \right) + \frac{x - 1}{(\lambda + 2\mu)},$$

and the pressure by

$$p(x, t) = -\frac{1}{\rho k} \sum_{n=0}^{\infty} \frac{2}{m_n \sqrt{d_n}} \sin(m_n x) e^{-at} \sin(\sqrt{d_n} t),$$

where, for $n \geq 0$,

$$a = \frac{1}{2\rho k}, \quad m_n = \frac{\pi + 2n\pi}{2}, \quad b_n = \frac{2}{(\lambda + 2\mu)m_n^2}, \quad d_n = \frac{(\lambda + 2\mu)}{\rho} m_n^2 - a^2. \tag{2.5}$$

Figure 1 shows the pressure solution when

$$\lambda = \mu = 1.32 \times 10^7 \text{ N/m}^2, \quad \rho = 1.7 \times 10^3 \text{ Kg/m}^3, \tag{2.6}$$

and the hydraulic conductivity is taken as $k = 10^{-5}$ m/s.

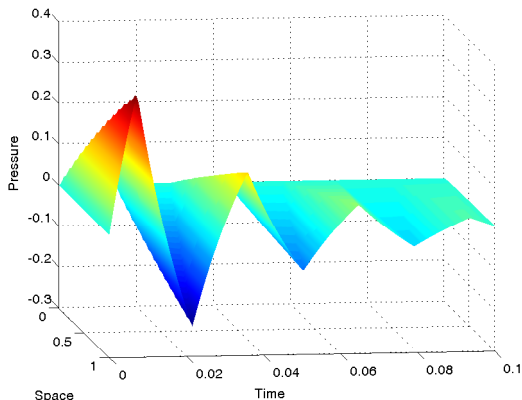


Figure 1. An accurate enough approximation for pressure obtained truncating the series of the analytical solution in a particular case $k\pi\sqrt{\rho(\lambda + 2\mu)} - 1 > 0$.

If $k\pi\sqrt{\rho(\lambda + 2\mu)} - 1 = 0$ we are in a transition case, however from the numerical point of view, the most interesting situation appears for small conductivities, and it corresponds to the relation $k\pi\sqrt{\rho(\lambda + 2\mu)} - 1 < 0$, where the analytical solution is given by

$$u(x, t) = \sum_{n=0}^{N_0-1} b_n \cos(m_n x) e^{-at} \left(\cosh(\sqrt{-d_n} t) + \frac{a}{\sqrt{-d_n}} \sinh(\sqrt{-d_n} t) \right) - \sum_{n=N_0}^{\infty} b_n \cos(m_n x) e^{-at} \left(\cos(\sqrt{d_n} t) + \frac{a}{\sqrt{d_n}} \sin(\sqrt{d_n} t) \right) + \frac{x - 1}{(\lambda + 2\mu)}$$

for displacements and by

$$p(x, t) = -\frac{1}{\rho k} \left(\sum_{n=0}^{N_0-1} \frac{2}{m_n \sqrt{-d_n}} \sin(m_n x) e^{-at} \sinh(\sqrt{-d_n} t) + \sum_{n=N_0}^{\infty} \frac{2}{m_n \sqrt{d_n}} \sin(m_n x) e^{-at} \sin(\sqrt{d_n} t) \right)$$

for the pressure, with N_0 the smallest integer such that $(1/(k\sqrt{\rho(\lambda + 2\mu)}) - \pi) < 2\pi N_0$ and a, m_n, b_n and d_n defined as in (2.5).

In this context, as it happens when a load is applied on an elastic saturated porous medium and inertial effects are neglected, the pressure quickly rises and sharp boundary layers in both space and time appear. In Figure 2, we display a particular example of this phenomenon choosing λ, μ, ρ as in (2.6), and $k = 10^{-9}$ m/s to be in the last case. Classical discretization methods may not be stable in the sense that strong non-physical oscillations appear in the approximated numerical solutions.

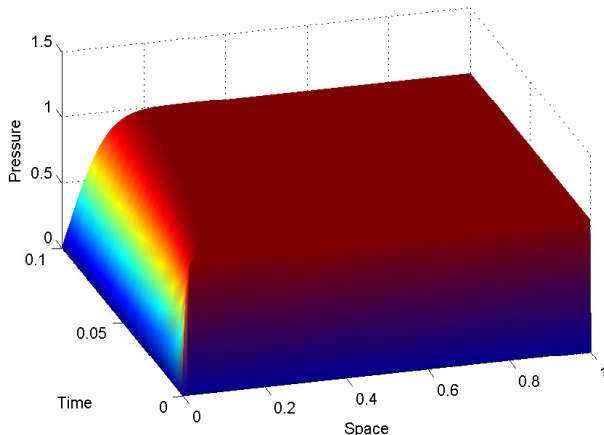


Figure 2. An accurate enough approximation for pressure in the case $\kappa\pi\sqrt{\rho(\lambda + 2\mu)} < 1$ obtained truncating the series of the analytical solution.

2.1 Standard discretization

For simplicity in the analysis, we will take uniform meshes both in space and time. Let N be a positive integer, we define $h = 1/N$ as space mesh size and denote by $x_i = ih, i = 0, \dots, N$ the mesh points. In the same way, let M be a positive integer, and we will also consider a uniform grid in the time domain $[0, T]$ with step $\tau = T/M$. Now, for each time level $t_m = m\tau, m = 1, \dots, M - 1$, we approximate the solution of the column problem with the standard finite-difference scheme

$$\begin{aligned} \rho(u_{h,\bar{t}t})_i^m - \frac{(\lambda + 2\mu)}{2} ((u_{h,\bar{x}x})_i^{m+1} + (u_{h,\bar{x}x})_i^m) + (p_{h,\bar{x}})_i^{m+1} &= 0, \\ (u_{h,t\bar{x}})_i^m - k(p_{h,\bar{x}x})_i^{m+1} &= 0, \end{aligned} \quad (2.7)$$

where (u_h, p_h) are grid functions denoting the numerical approximation to (u, p) . We use the standard index-free notation for finite difference schemes [8]. Scheme (2.7) must be completed with suitable boundary and initial conditions. If we approach the solution of the column problem (2.1)–(2.4) by discretization (2.7), the behaviour of the numerical solution depends on the chosen material parameters. If we choose the values given in (2.6) and $k = 10^{-5}$, even though the analytical solution has a marked oscillatory behaviour, it can be satisfactorily approximated taking a small enough step size to capture the oscillatory behaviour (see Figures 3 and 4).

However, if we change the hydraulic conductivity to $k = 10^{-9}$, the column problem is not satisfactorily solved by (2.7), because spurious oscillations for displacement and pressure approximations appear. This phenomenon can be observed in Figures 5 and 6 where we display a comparison between the analytical solution and the numerical approximation, for displacements and pressure respectively, at time $T = 0.001$ with $N = M = 20$.

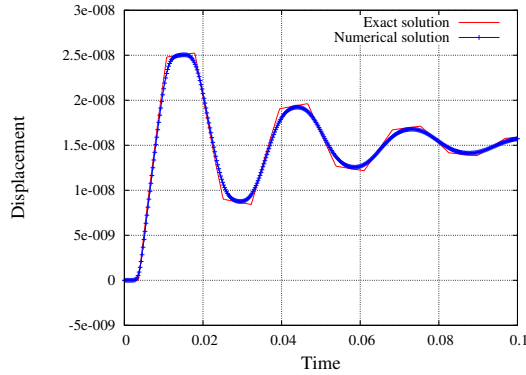


Figure 3. Time history for an accurate enough approximation of the analytical solution and a numerical solution for displacements, obtained by scheme (2.7) for the column problem with $N = M = 400$ at node $x = 0.5$.

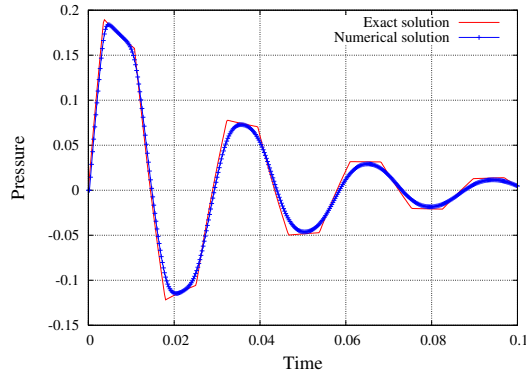


Figure 4. Time history for an accurate enough approximation of the analytical solution and a numerical solution for pressure, obtained by scheme (2.7) for the column problem with $N = M = 400$ at node $x = 0.5$.

2.2 Stabilization of scheme (2.7)

In this simple 1D test problem, system (2.1)–(2.4) can be decoupled. From the second differential equation and boundary conditions on $x = 1$, we obtain the relation

$$\frac{\partial p}{\partial x} = \frac{1}{k} \frac{\partial u}{\partial t}. \tag{2.8}$$

By substituting this expression into the first equation, the original problem can be written as

$$\begin{aligned} \rho \frac{\partial^2 u}{\partial t^2} - (\lambda + 2\mu) \frac{\partial^2 u}{\partial x^2} + \frac{1}{k} \frac{\partial u}{\partial t} &= 0, \\ \frac{\partial p}{\partial x} - \frac{1}{k} \frac{\partial u}{\partial t} &= 0, \quad x \in (0, 1), \quad 0 < t < T \end{aligned} \tag{2.9}$$

subject to the boundary and initial conditions (2.2)–(2.4).

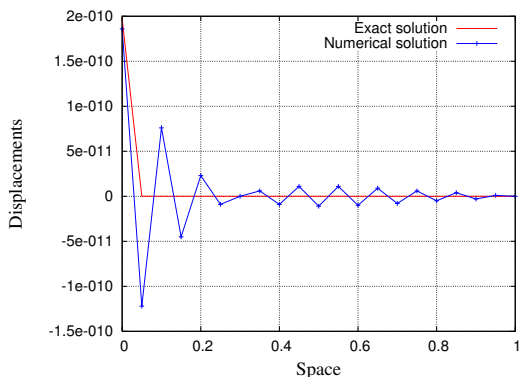


Figure 5. Comparison between an accurate enough approximation of the analytical solution and an approximated solution for displacements, obtained by scheme (2.7) for the column problem at time $T = 0.001$ and $N = M = 20$.

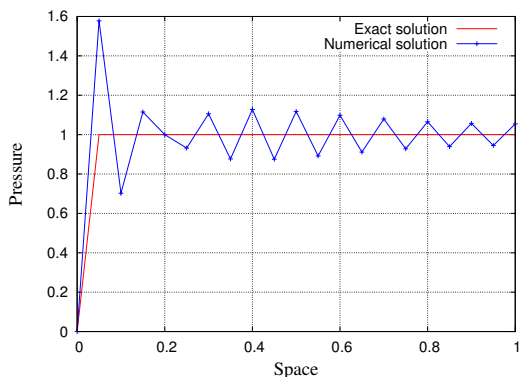


Figure 6. Comparison between an accurate enough approximation of the analytical solution and an approximated solution for pressure obtained by scheme (2.7) for the column problem at time $T = 0.001$ and $N = M = 20$.

Now, for $i = 1, \dots, N - 1$ and $m = 1, \dots, M - 1$, the numerical solution of the column problem can be performed using for the first equation of (2.9) the following scheme

$$\rho(u_{h,\bar{t}t})_i^m - \frac{(\lambda + 2\mu)}{2} ((u_{h,\bar{x}x})_i^{m+1} + (u_{h,\bar{x}x})_i^m) + \frac{1}{k} (u_{h,t})_i^m = 0 \quad (2.10)$$

with a suitable approximation of initial and boundary conditions for displacements.

It is clear that the numerical solution for the uncoupled formulation of the column problem, does not present any numerical instabilities, independently of the choice of h and τ , because the resulting coefficient matrices are M-matrices in each time level.

Now, we decouple scheme (2.7) in order to compare it with the previous scheme (2.10). Taking into account the boundary conditions, at each time

level, we obtain the relations

$$p_{h,N+1}^m = p_{h,N-1}^m, \quad (u_{h,t})_{N+1}^m = -(u_{h,t})_{N-1}^m,$$

where a ghost point x_{N+1} has been considered in the space grid. Then, the second equation of (2.7) in the node x_N gives

$$(u_{h,t})_{N-1}^m = 2k \left(\frac{p_{h,N}^{m+1} - p_{h,N-1}^{m+1}}{h} \right).$$

Since, $(u_{h,t})_N^m = 0$, we have

$$\frac{(u_{h,t})_N^m + (u_{h,t})_{N-1}^m}{2} = k \left(\frac{p_{h,N}^{m+1} - p_{h,N-1}^{m+1}}{h} \right). \quad (2.11)$$

In a similar way, for $i = N - 1, \dots, 1$, rewriting the second equation of (2.7) in each internal node x_i and applying recursion, we deduce the following relation

$$\frac{(u_{h,t})_i^m + (u_{h,t})_{i-1}^m}{2} = k \left(\frac{p_{h,i}^{m+1} - p_{h,i-1}^{m+1}}{h} \right), \quad (2.12)$$

and then

$$\left(\frac{(u_{h,t})_{i+1}^m + 2(u_{h,t})_i^m + (u_{h,t})_{i-1}^m}{4} \right) = k \frac{p_{h,i+1}^{m+1} - p_{h,i-1}^{m+1}}{2h}. \quad (2.13)$$

Then, the first equation of (2.7) can be rewritten as

$$\rho(u_{h,\bar{t}\bar{t}})_i^m - \frac{(\lambda + 2\mu)}{2} \left((u_{h,\bar{x}\bar{x}})_i^{m+1} + (u_{h,\bar{x}\bar{x}})_i^m \right) + \frac{1}{k} (\widehat{u_{h,t}})_i^m = 0, \quad (2.14)$$

where

$$\widehat{v}_{h,i}^m := \left(\frac{v_{h,i+1}^m + 2v_{h,i}^m + v_{h,i-1}^m}{4} \right)$$

gives us a second order approximation of $v_{h,i}^m$.

Solving (2.14), for each time level a linear system appears with equations

$$\begin{aligned} & \left(c + \frac{\tau}{4k} \right) u_{h,i-1}^{m+1} + \left(\rho - 2c + \frac{\tau}{2k} \right) u_{h,i}^{m+1} + \left(c + \frac{\tau}{4k} \right) u_{h,i+1}^{m+1} \\ & = 2\rho u_{h,i}^m + \rho u_{h,i}^{m-1} - c(u_{h,i+1}^m - 2u_{h,i}^m + u_{h,i-1}^m) + \frac{\tau}{k} \widehat{u}_{h,i}^m, \end{aligned} \quad (2.15)$$

where $c = -(\lambda + 2\mu)\tau^2/(2h^2)$.

Now, the extradiagonal elements $c + \frac{\tau}{4k}$ can be positive, depending on h and τ , and spurious oscillations come from the positivity of these coefficients. So, if $h^2 < 2k(\lambda + 2\mu)\tau$, the tridiagonal matrices obtained from (2.15) are M-matrices. Therefore this unstable behaviour can be avoided taking a small enough spatial discretization step. However, when we consider a small time step in the initial stage, this restriction on the mesh size is severe and a big computational effort can be required for multidimensional problems.

It is worth to compare finite difference scheme (2.10) for the decoupled problem and the decoupled scheme (2.14). It can be observed that the only

discrepancy appears in the approximation of $\partial u/\partial t$. In the first case, to approximate $\partial u/\partial t(x_i, t_m)$ we use the forward difference $(u_{h,t})_i^m$, whereas, in the second one, we take $(\widehat{u}_{h,t})_i^m$ that is an average in neighbouring points. The following relation is satisfied

$$(\widehat{u}_{h,t})_i^m - (u_{h,t})_i^m = \left(\frac{(u_{h,t})_{i+1}^m - 2(u_{h,t})_i^m + (u_{h,t})_{i-1}^m}{4} \right) = \frac{h^2}{4} ((u_{h,t})_{\bar{x}x})_i^m. \tag{2.16}$$

So, a possible way to stabilize (2.7) is to perturb the displacement equation in order to recover scheme (2.10).

Coming back to the column problem, we approach its solution over a uniform grid in space with step size h and a uniform grid in $[0, T]$ with time step τ , in the following way

$$\begin{aligned} \rho(u_{h,\bar{t}\bar{t}})_i^m - \frac{(\lambda + 2\mu)}{2} ((u_{h,\bar{x}x})_i^{m+1} + (u_{h,\bar{x}x})_i^m) + (p_{h,\bar{x}})_i^{m+1} - \frac{h^2}{4k} ((u_{h,t})_{\bar{x}x})_i^m &= 0, \\ (u_{h,t\bar{x}})_i^m - k(p_{h,\bar{x}x})_i^{m+1} &= 0. \end{aligned} \tag{2.17}$$

3 The General Case

3.1 Fully discrete problem

For simplicity, we restrict ourselves to the two-dimensional case. All results presented here, can be straightforwardly generalized to the three-dimensional case. Although more general conditions can be considered, for simplicity we focus on the fully dynamic Biot's model given by (1.1) on a square unit domain Ω of side L with homogeneous Dirichlet boundary conditions

$$\mathbf{u}(\mathbf{x}, t) = 0, \quad p(\mathbf{x}, t) = 0, \quad \mathbf{x} \in \partial\Omega, \quad t > 0 \tag{3.1}$$

and initial conditions

$$\mathbf{u}(\mathbf{x}, 0) = \mathbf{u}^0(\mathbf{x}), \quad \frac{\partial \mathbf{u}}{\partial t}(\mathbf{x}, 0) = \mathbf{w}^0(\mathbf{x}), \quad p(\mathbf{x}, 0) = p^0(\mathbf{x}), \quad \mathbf{x} \in \Omega, \tag{3.2}$$

and we restrict our attention to the case of very small conductivities leading to a over-damped wave.

Let N be a positive integer, $h = L/N$ the mesh size and $\bar{\omega}$ the set of nodes $\bar{\omega} = \{(ih, jh), i, j = 0, 1, \dots, N\}$, ω denotes the internal nodes and $\partial\bar{\omega}$ the set of boundary grid points. We define the corresponding Hilbert spaces of grid functions $H_{\bar{\omega}}$ and $\bar{\mathbf{H}} = H_{\bar{\omega}} \times H_{\bar{\omega}}$, with usual L_2 inner product [8]. We also denote by H_ω and $\mathbf{H} = H_\omega \times H_\omega$ the subspaces of grid functions vanishing on the boundaries.

Now, we discretize the divergence operator by the second order approximation $D\mathbf{v} = (v_1)_{x_1}^\circ + (v_2)_{x_2}^\circ$ for $\mathbf{v} \in \mathbf{H}$. The discrete gradient operator $G : H_\omega \rightarrow \mathbf{H}$ is taken such that $(Gy, \mathbf{w}) = -(y, D\mathbf{w})$, i.e., as the negative adjoint to operator D .

To discretize the elasticity operator, we use the operator $A : \mathbf{H} \rightarrow \mathbf{H}$ given by $A = -\mu\Delta_h - (\lambda + \mu)GD$ where $\Delta_h = \text{diag}(\Delta_h, \Delta_h)$, and $\Delta_h v = v_{\bar{x}_1 x_1} + v_{\bar{x}_2 x_2}$

is the usual five-point stencil approximation of the scalar Laplace operator. Operator A is self-adjoint and positive definite on \mathbf{H} , i.e. $A = A^* \geq \delta_A \mathbf{E}$ where $\delta_A > 0$ is independent of h and \mathbf{E} is the identity operator in \mathbf{H} .

Finally, the discrete diffusion operator $B : H_\omega \rightarrow H_\omega$ is defined by $By = -k\Delta_h y$, so that B is symmetric and positive definite in H_ω , i.e., $B = B^* \geq \delta_B E$ where $\delta_B > 0$ is independent of h and E is the identity operator in H_ω .

The semi-discrete approximations $\mathbf{u}_h(t) \in \mathbf{H}$ and $p_h(t) \in H$ are given by the solution of the Cauchy problem

$$\begin{aligned} \rho \frac{d^2 \mathbf{u}_h(t)}{dt^2} + A\mathbf{u}_h(t) + \alpha G p_h(t) &= \mathbf{g}_h(t), \\ \frac{d}{dt} (\gamma p_h(t) + \alpha D\mathbf{u}_h(t)) + Bp_h(t) &= f_h(t) \end{aligned} \tag{3.3}$$

for all $t \in (0, T]$, with initial conditions

$$\mathbf{u}_h(0) = \mathbf{u}_h^0, \quad \frac{d}{dt} \mathbf{u}_h(0) = \mathbf{w}_h^0, \quad p_h(0) = p_h^0. \tag{3.4}$$

For time discretization of (3.3)–(3.4), we consider a uniform grid in $[0, T]$. Let \mathbf{u}_h^m and p_h^m be approximations to $\mathbf{u}_h(t_m)$ and $p_h(t_m)$, where $t_m = m\tau$, $m = 0, 1, \dots, M$ and $T = \tau M$. Generalizing (2.7) to the two-dimensional case, we propose a stabilized finite-difference scheme based on the perturbation of the equation for the displacements. Namely, we define the discrete operator $C : \mathbf{H} \rightarrow \mathbf{H}$ as

$$C = (-h^2/4k) \widetilde{\Delta}_h, \tag{3.5}$$

which is self-adjoint and positive definite on \mathbf{H} and, for $m = 1, \dots, M - 1$, we approach the solution of the fully dynamic Biot’s problem by

$$\begin{aligned} \rho \frac{\mathbf{w}_h^{m+1} - \mathbf{w}_h^m}{\tau} + A \frac{\mathbf{u}_h^{m+1} + \mathbf{u}_h^m}{2} + \alpha G p_h^{m+1} + C \mathbf{w}_h^{m+1} &= \mathbf{g}_h^m, \\ \gamma \frac{p_h^{m+1} - p_h^m}{\tau} + \alpha D \mathbf{w}_h^{m+1} + B p_h^{m+1} &= f_h^{m+1} \end{aligned} \tag{3.6}$$

with $\mathbf{w}_h^{m+1} = (\mathbf{u}_h^{m+1} - \mathbf{u}_h^m)/\tau$.

3.2 Stability and convergence

Proposition 1. *The solution of difference scheme (3.6) satisfies the a priori estimate*

$$\begin{aligned} \rho \|\mathbf{w}_h^{m+1}\|^2 + \|\mathbf{u}_h^{m+1}\|_A^2 + \gamma \|p_h^{m+1}\|^2 &\leq \frac{\tau}{2} (\widetilde{K}_1 \|\mathbf{g}_h^m\|^2 + \widetilde{K}_2 \|f_h^{m+1}\|_{B^{-1}}^2) \\ &+ \widetilde{K}_3 (\rho \|\mathbf{w}_h^m\|^2 + \|\mathbf{u}_h^m\|_A^2 + \gamma \|p_h^m\|^2) \end{aligned}$$

for $m = 1, 2, \dots, M - 1$, where \widetilde{K}_1 , \widetilde{K}_2 and \widetilde{K}_3 are constants independent of h and τ .

Proof. Multiplying the first equation of (3.6) by $(\tau \mathbf{w}_h^{m+1})$ and taking into account that $2(\mathbf{w}_h^{m+1} - \mathbf{w}_h^m, \mathbf{w}_h^{m+1}) \geq \|\mathbf{w}_h^{m+1}\|^2 - \|\mathbf{w}_h^m\|^2$, we obtain

$$\begin{aligned} & \frac{\rho}{2} \left(\|\mathbf{w}_h^{m+1}\|^2 - \|\mathbf{w}_h^m\|^2 \right) + \frac{1}{2} (\|\mathbf{u}_h^{m+1}\|_A^2 - \|\mathbf{u}_h^m\|_A^2) + \alpha (Gp_h^{m+1}, \tau \mathbf{w}_h^{m+1}) \\ & + \tau \|\mathbf{w}_h^{m+1}\|_C^2 \leq (\mathbf{g}_h^m, \tau \mathbf{w}_h^{m+1}). \end{aligned}$$

By the generalized Cauchy–Schwarz inequality, we have

$$\begin{aligned} & \frac{\rho}{2} (\|\mathbf{w}_h^{m+1}\|^2 - \|\mathbf{w}_h^m\|^2) + \frac{1}{2} (\|\mathbf{u}_h^{m+1}\|_A^2 - \|\mathbf{u}_h^m\|_A^2) + \alpha (Gp_h^{m+1}, \tau \mathbf{w}_h^{m+1}) \\ & \leq \frac{\rho}{2} (1 - e^{-\beta\tau}) \|\mathbf{w}_h^{m+1}\|^2 + \frac{\tau^2}{2\rho(1 - e^{-\beta\tau})} \|\mathbf{g}_h^m\|^2 \end{aligned} \tag{3.7}$$

with $\beta > 0$. Next, if we consider the second equation of (3.6) and we multiply it by (τp_h^{m+1}) we obtain

$$\frac{\gamma}{2} (\|p_h^{m+1}\|^2 - \|p_h^m\|^2) + \alpha (D\mathbf{w}_h^{m+1}, \tau p_h^{m+1}) \leq \frac{\tau}{4} \|f_h^{m+1}\|_{B^{-1}}^2. \tag{3.8}$$

From (3.7) and (3.8),

$$\begin{aligned} & \rho e^{-\beta\tau} \|\mathbf{w}_h^{m+1}\|^2 + \|\mathbf{u}_h^{m+1}\|_A^2 + \gamma \|p_h^{m+1}\|^2 \\ & \leq \rho \|\mathbf{w}_h^m\|^2 + \|\mathbf{u}_h^m\|_A^2 + \gamma \|p_h^m\|^2 + \frac{\tau}{2} \|f_h^{m+1}\|_{B^{-1}}^2 + \frac{\tau^2}{\rho(1 - e^{-\beta\tau})} \|\mathbf{g}_h^m\|^2. \end{aligned}$$

Then, as $\beta > 0$, it is fulfilled

$$\begin{aligned} \rho \|\mathbf{w}_h^{m+1}\|^2 + \|\mathbf{u}_h^{m+1}\|_A^2 + \gamma \|p_h^{m+1}\|^2 & \leq e^{\beta\tau} (\rho \|\mathbf{w}_h^m\|^2 + \|\mathbf{u}_h^m\|_A^2 + \gamma \|p_h^m\|^2) \\ & + \frac{\tau}{2} \left(e^{\beta\tau} \|f_h^{m+1}\|_{B^{-1}}^2 + \frac{2e^{2\beta\tau}}{\rho\beta} \|\mathbf{g}_h^m\|^2 \right), \end{aligned} \tag{3.9}$$

and final estimate results. \square

The convergence results follow from the error-problem

$$\begin{aligned} & \rho \frac{\delta \mathbf{u}_h^{m+1} - 2\delta \mathbf{u}_h^m + \delta \mathbf{u}_h^{m-1}}{\tau^2} + A \frac{\delta \mathbf{u}_h^{m+1} + \delta \mathbf{u}_h^m}{2} + \alpha G \delta p_h^{m+1} \\ & + C \frac{\delta \mathbf{u}_h^{m+1} - \delta \mathbf{u}_h^m}{\tau} = \Psi_h^m, \\ & \gamma \frac{\delta p_h^{m+1} - \delta p_h^m}{\tau} + \alpha \frac{D \delta \mathbf{u}_h^{m+1} - D \delta \mathbf{u}_h^m}{\tau} + B \delta p_h^{m+1} = \phi_h^m, \end{aligned} \tag{3.10}$$

where

$$\delta \mathbf{u}_h^m = \mathbf{u}_h^m - \mathbf{u}(\cdot, t_m) \in \mathbf{H}, \quad \delta p_h^m := p_h^m - p(\cdot, t_m) \in H_\omega,$$

for $m = 1, \dots, M$, and the right-hand side functions Ψ_h^m and ϕ_h^m are the approximation errors given by

$$\begin{aligned} \Psi_h^m(\mathbf{x}) &= \rho \frac{\mathbf{u}(\mathbf{x}, t_{m+1}) - 2\mathbf{u}(\mathbf{x}, t_m) + \mathbf{u}(\mathbf{x}, t_{m-1}))}{\tau^2} + \alpha Gp(\mathbf{x}, t_{m+1}) \\ &\quad + A \frac{\mathbf{u}(\mathbf{x}, t_{m+1}) + \mathbf{u}(\mathbf{x}, t_m)}{2} + C \frac{\mathbf{u}(\mathbf{x}, t_{m+1}) - \mathbf{u}(\mathbf{x}, t_m)}{\tau} - \mathbf{g}_h(\mathbf{x}, t_m), \quad \mathbf{x} \in \omega, \\ \phi_h^m(\mathbf{x}) &= \gamma \frac{p(\mathbf{x}, t_{m+1}) - p(\mathbf{x}, t_{m-1}))}{2\tau} + \alpha \frac{D\mathbf{u}(\mathbf{x}, t_{m+1}) - D\mathbf{u}(\mathbf{x}, t_{m-1}))}{2\tau} \\ &\quad + Bp(\mathbf{x}, t_{m+1}) - f_h(\mathbf{x}, t_m), \quad \mathbf{x} \in \omega. \end{aligned}$$

If the exact solution is smooth enough, it is easy to verify by simple Taylor expansion that $\Psi_h^m(\mathbf{x}) = \mathcal{O}(h^2 + \tau)$, and $\phi_h^m(\mathbf{x}) = \mathcal{O}(h^2 + \tau)$ for $\mathbf{x} \in \omega$.

From the stability results given in Proposition 1, we can prove the next convergence result.

Proposition 2. *Let $\mathbf{u}(\mathbf{x}, t)$ and $p(\mathbf{x}, t)$ be the solution of problem (1.1) with (3.1)–(3.2) as boundary and initial condition and let $(\mathbf{u}_h^{m+1}, \mathbf{w}_h^{m+1}, p_h^{m+1})$ be the numerical solution of finite difference scheme (3.6). If $\mathbf{u}_h^1, \mathbf{w}_h^1$ and p_h^1 are $\mathcal{O}(h^2 + \tau)$ approximations of $\mathbf{u}(\mathbf{x}, \tau)$, $\frac{\partial \mathbf{u}}{\partial t}(\mathbf{x}, \tau)$ and $p(\mathbf{x}, \tau)$, then*

$$\rho \|\delta \mathbf{w}_h^{m+1}\| + \|\delta \mathbf{u}_h^{m+1}\|_A + \gamma \|\delta p_h^{m+1}\| = \mathcal{O}(h^2 + \tau).$$

Proof. By using estimate (3.9) recursively, we have

$$\begin{aligned} &\rho \|\delta \mathbf{w}_h^{m+1}\|^2 + \|\delta \mathbf{u}_h^{m+1}\|_A^2 + \gamma \|\delta p_h^{m+1}\|^2 \\ &\leq e^{\beta\tau m} (\rho \|\delta \mathbf{w}_h^1\|^2 + \|\delta \mathbf{u}_h^1\|_A^2 + \gamma \|\delta p_h^1\|^2) \\ &\quad + \frac{\tau}{2} \sum_{k=1}^m e^{\beta\tau(m-k)} \left(\frac{2e^{2\beta\tau}}{\rho\beta} \|\Psi_h^k\|^2 + e^{\beta\tau} \|\phi_h^{k+1}\|_{B^{-1}}^2 \right) \\ &\leq e^{3\beta T} \left(\rho \|\delta \mathbf{w}_h^1\|^2 + \|\delta \mathbf{u}_h^1\|_A^2 + \gamma \|\delta p_h^1\|^2 + \frac{\tau}{2} \sum_{k=1}^m \left(\frac{2}{\rho\beta} \|\Psi_h^k\|^2 + \|\phi_h^{k+1}\|_{B^{-1}}^2 \right) \right). \end{aligned}$$

The result follows taking into account the previous bounds for the approximation errors Ψ_h^m and ϕ_h^{m+1} . \square

4 Numerical Experiments for the Stabilized Scheme

In this section, numerical experiments confirming the theoretical results are presented. First, we consider again the one-dimensional test problem described in the Section 2 and we analyze numerical results obtained when we approach its solution with the perturbed finite-difference scheme (2.17). To finish, we present numerical experiments for a 2D problem.

4.1 The column problem

Now, we consider the 1D test problem (2.1)–(2.4) previously defined in Section 2. We choose the material parameters λ, μ, ρ given in (2.6) and we

consider a small conductivity case taking $k = 10^{-9}$, so $k\pi\sqrt{\rho(\lambda + 2\mu)} - 1 < 0$ yields. In this situation, a sharp boundary layer in both space and time appears in the pressure field.

In Table 1, we display the energy norm of the errors for displacements and the L_2 -norm for the pressure, i.e., $\|\delta u_h\|_A$ and $\|\delta p_h\|$, for $T = 0.1$ and several values of parameters N and M . We check that these numerical results are in agreement with the theory proved in this paper.

Table 1. Errors in energy norm for displacements and L_2 -norm for pressure at time $T = 0.1$ by using the perturbed finite-difference scheme (2.17).

Space	Time	$\ \delta u_h\ _A$	$\ \delta p_h\ $
$N = 40$	$M = 10$	3.5670×10^{-10}	1.1701×10^{-2}
$N = 80$	$M = 20$	1.4425×10^{-10}	5.7668×10^{-3}
$N = 160$	$M = 40$	6.4507×10^{-11}	2.8619×10^{-3}
$N = 320$	$M = 80$	3.0461×10^{-11}	1.4260×10^{-3}

In Figures 7 and 8, we represent the numerical solution for displacements and pressure fields for $T = 0.001$ when we use (3.6) with $N = M = 20$. In this case, any non-physical oscillation is observed in the behaviour of the numerical approximations of displacement and pressure fields.

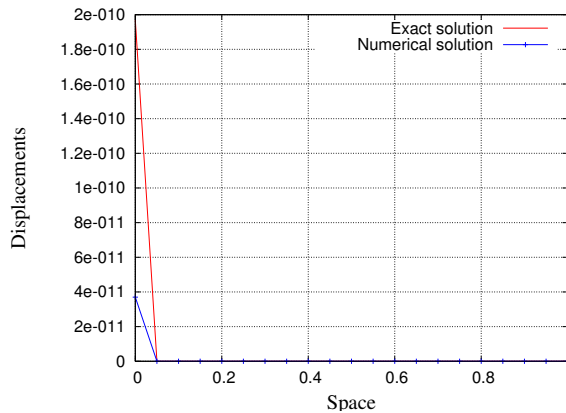


Figure 7. Comparison between an accurate enough approximation of the analytical solution and an approximated solution for displacements obtained by perturbed scheme (3.6) for the column problem at time $T = 0.001$ and $N = M = 20$.

This way to stabilize the problem by perturbing an equation is usual in incompressible Navier–Stokes equations, adding for example the term $ah^2\Delta_h p_h$ to the divergence constraint equation. In this case, a big limitation appears because the strategy requires a “good” choice of the stabilization parameter a . It is very easy to over-stabilize by using a parameter value that is too large. This is not the case here. As we are going to see, the obtained parameter $h^2/(4k)$ is the best, at least for the one-dimensional case on a uniform grid. To

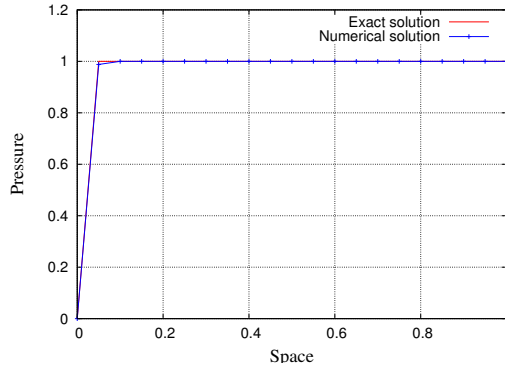


Figure 8. Comparison between an accurate enough approximation of the analytical solution and an approximated solution for pressure obtained by perturbed scheme (3.6) for the column problem at time $T = 0.001$ and $N = M = 20$.

confirm this numerically, we consider the perturbed scheme

$$\begin{aligned} \rho \frac{\mathbf{u}_h^{m+1} - 2\mathbf{u}_h^m + \mathbf{u}_h^{m-1}}{\tau^2} + A \frac{\mathbf{u}_h^{m+1} + \mathbf{u}_h^m}{2} + \alpha G p_h^{m+1} + C_\beta \frac{\mathbf{u}_h^{m+1} - \mathbf{u}_h^m}{\tau} &= \mathbf{g}_h^m, \\ \gamma \frac{p_h^{m+1} - p_h^m}{\tau} + \alpha \frac{D\mathbf{u}_h^{m+1} - D\mathbf{u}_h^m}{\tau} + B p_h^{m+1} &= f_h^{m+1}, \end{aligned} \tag{4.1}$$

where

$$C_\beta \frac{\mathbf{u}_h^{m+1} - \mathbf{u}_h^m}{\tau} := -\frac{\beta h^2}{4k} \widetilde{\Delta}_h \left(\frac{\mathbf{u}_h^{m+1} - \mathbf{u}_h^m}{\tau} \right)$$

with β a free parameter. If $\beta = 1$ we get the perturbed discrete problem (2.17), and if $\beta = 0$ we get the standard finite-difference scheme without perturbing. We consider the column problem for the small conductivity case, $k = 10^{-9}$.

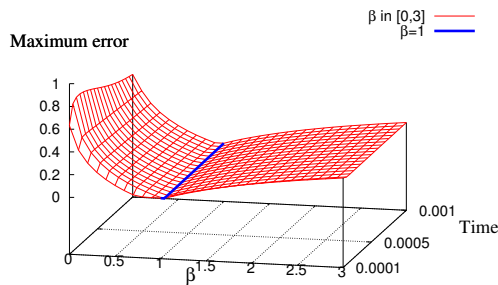


Figure 9. Maximum error obtained for different values of β for the column problem with $k = 10^{-9}$ and $N = M = 20$.

In Figure 9 we have represented the maximum error obtained in a time step for different values of $\beta \in [0, 3]$ and for different time step sizes. In accordance

with these results it can be observed that the minimum error is reached with our proposed stabilization parameter corresponding to $\beta = 1$.

4.2 A two-dimensional problem

The aim of this last experiment is to assess the good performance of the proposed stabilization for a two-dimensional realistic problem. It corresponds to a 2D elastic soil foundation subjected to a surface step loading of $\sigma_0 = 10^3 \text{ N/m}^2$. The simulation domain is a 10 by 10 meters block of porous soil, $\Omega = (-5, 5) \times (0, 10)$, as in Figure 10.

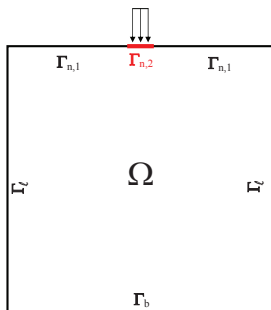


Figure 10. Computational domain for the two-dimensional numerical experiment.

At the base of this domain the soil is assumed to be fixed, i.e. both horizontal and vertical components of displacements are taken as zero, while at some centered upper part of the domain a uniform load is applied in a strip of length $1m$ as depicted in Figure 10.

The remaining of the top surface is assumed to be traction free. Horizontal displacement and vertical surface traction are assumed to be zero on each of the vertical walls. Concerning the pressure, we prescribe the pore pressure at the top surface as zero, and we assume the lateral and the bottom boundaries to be impermeable. More precisely, the boundary condition is given as follows

$$\begin{aligned}
 p &= 0, & \sigma_{xy} &= 0, & \sigma_{yy} &= 0, & \text{on } \Gamma_{n,1}, \\
 p &= 0, & \sigma_{xy} &= 0, & \sigma_{yy} &= -\sigma_0, & \text{on } \Gamma_{n,2}, \\
 \frac{\partial p}{\partial n} &= 0, & \sigma_{xy} &= 0, & u &= 0, & \text{on } \Gamma_l, \\
 \frac{\partial p}{\partial n} &= 0, & v &= 0, & u &= 0, & \text{on } \Gamma_b,
 \end{aligned}$$

where $\sigma_{xy} = \mu \left(\frac{\partial u}{\partial y} + \frac{\partial v}{\partial x} \right)$, $\sigma_{yy} = \lambda \frac{\partial u}{\partial x} + (\lambda + 2\mu) \frac{\partial v}{\partial y}$, and

$$\begin{aligned}
 \Gamma_{n,1} &= \{(x, y) \in \partial\Omega \mid |x| > 1/2, y = 10\}, \\
 \Gamma_{n,2} &= \{(x, y) \in \partial\Omega \mid |x| \leq 1/2, y = 10\}, \\
 \Gamma_l &= \{(x, y) \in \partial\Omega \mid |x| = 5\}, & \Gamma_b &= \{(x, y) \in \partial\Omega \mid y = 0\}.
 \end{aligned}$$

The material properties of the porous medium are indicated in Table 2 where λ and μ are related to the Young's modulus E and the Poisson's ratio ν by

$$\lambda = \frac{\nu E}{(1 + \nu)(1 - 2\nu)}, \quad \mu = \frac{E}{2(1 + \nu)}.$$

Table 2. Material parameters for the two-dimensional problem.

Parameter	Definition	Value	Unit
E	Young's modulus	3.3×10^7	N/m ²
ν	Poisson's ratio	0.25	–
ρ	Density of the soil	1.7×10^3	Kg/m ³
k	Hydraulic conductivity	10^{-9}	m/s

A mesh consisting of 101×101 nodes is used in the numerical experiment. In order to adequately capture the time boundary layer, we have chosen the final time $T = 0.001$ and the number of subdivisions in time $M = 2$. Figure 11 shows that the approximation of the first derivatives by standard central differences lead to spurious oscillations in the pressure at time $T = 10^{-3}$.

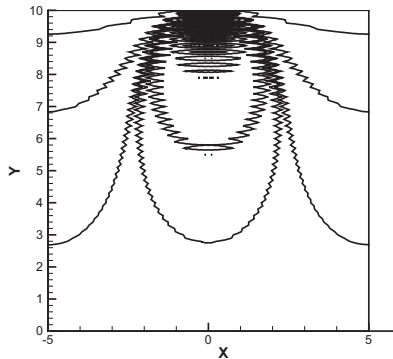


Figure 11. Pressure contours for the two-dimensional problem without stabilization term.

These unphysical oscillations in the pressure are eliminated completely adding the stabilization term to the first equation as can be seen in Figure 12.

5 Conclusions

In this paper we have presented a stabilized finite difference scheme for the incompressible fully dynamic poroelastic model. Stabilization is done by adding an extra term to the equilibrium equation, that permits us to use central difference schemes to approximate the first order spatial derivatives providing numerical solutions without oscillations independently of the chosen discretization parameters. The stabilization parameter depends on the mesh size and the

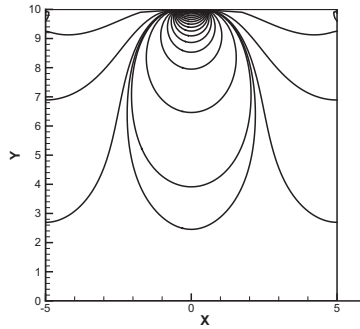


Figure 12. Pressure contours for the two-dimensional problem adding the stabilization term.

properties of the porous medium. In the one-dimensional case, this parameter is shown to be optimal.

References

- [1] G. Aguilar, F. Gaspar, F. Lisbona and C. Rodrigo. Numerical stabilization of Biot's consolidation model by a perturbation on the flow equation. *Int. J. Numer. Meth. Engng.*, **75**:1282–1300, 2008. <http://dx.doi.org/10.1002/nme.2295>.
- [2] H. Barucq, M. Madaune-Tort and P. Saint-Macary. On nonlinear Biot's consolidation models. *Nonlinear Anal.*, **63**:985–995, 2005. <http://dx.doi.org/10.1016/j.na.2004.12.010>.
- [3] M. Biot. General solutions of the equations of elasticity and consolidation of a porous material. *J. Appl. Phys.*, **23**:91–96, 1956.
- [4] N. Boal, F.J. Gaspar, F.J. Lisbona and P.N. Vabishchevich. Finite-difference analysis of fully dynamic problems for saturated porous media. *J. Comput. Appl. Math.*, **236**:1090–1102, 2011. <http://dx.doi.org/10.1016/j.cam.2011.07.032>.
- [5] N. Boal, F.J. Gaspar, F.J. Lisbona and P.N. Vabishchevich. Finite-difference analysis of a double-porosity consolidation model. *Numer. Methods Partial Differential Equations*, **28**:138–154, 2012. <http://dx.doi.org/10.1002/num.20612>.
- [6] F.J. Gaspar, F.J. Lisbona and P.N. Vabishchevich. Staggered grid discretizations for the quasi-static Biot's consolidation problem. *Appl. Num. Math.*, **56**:888–898, 2006. <http://dx.doi.org/10.1016/j.apnum.2005.07.002>.
- [7] M. Pastor, T. Li and J.A.F. Merodo. Stabilized finite elements for harmonic soil dynamics problems near the undrained-incompressible limit. *Soil Dyn. Earthq. Eng.*, **16**:161–171, 1997. [http://dx.doi.org/10.1016/S0267-7261\(97\)00046-8](http://dx.doi.org/10.1016/S0267-7261(97)00046-8).
- [8] A.A. Samarskii. *The Theory of Difference Schemes*. Marcel Dekker Inc., New York, Basel, 2001.
- [9] O.C. Zienkiewicz, C.T. Chang and P. Bettles. Drained undrained consolidating and dynamic behaviour assumptions in soils. *Geotechnique*, **30**(4):385–395, 1980. <http://dx.doi.org/10.1680/geot.1980.30.4.385>.
- [10] O.C. Zienkiewicz, M. Huang and M. Pastor. Computational soil dynamics—A new algorithm for drained and undrained conditions. *Computational Methods in Advanced Geomechanics*, pp. 47–59, 1994.